The Journal of Experimental Biology 211, 3433-3441
Published by The Company of Biologists 2008
doi:10.1242/jeb.020495

To break a coralline: mechanical constraints on the size and survival of a wave-swept seaweed

Patrick T. Martone* and Mark W. Denny

Hopkins Marine Station of Stanford University, Pacific Grove, CA 93950, USA

*Author for correspondence at present address: Department of Botany, University of British Columbia, Vancouver, BC, Canada, V6T 1Z4
(e-mail: pmartone@interchange.ubc.ca)

Accepted 6 September 2008

SUMMARY

Previous studies have hypothesized that wave-induced drag forces may constrain the size of intertidal organisms by dislodging or breaking organisms that exceed some critical dimension. In this study, we explored constraints on the size of the articulated coralline alga *Calliarthron*, which thrives in wave-exposed intertidal habitats. Its ability to survive depends critically upon its segmented morphology (calcified segments separated by flexible joints or 'genicula'), which allows otherwise rigid fronds to bend and thereby reduce drag. However, bending also amplifies stress within genicula near the base of fronds. We quantified breakage of genicula in bending by applying known forces to fronds until they broke. Using a mathematical model, we demonstrate the mitigating effect of neighboring fronds on breakage and show that fronds growing within dense populations are no more likely to break in bending than in tension, suggesting that genicular morphology approaches an engineering optimum, possibly reflecting adaptation to hydrodynamic stress. We measured drag in a re-circulating water flume (0.23–3.6 m s^{-1}) and a gravity-accelerated water flume, which generates jets of water that mimic the impact of breaking waves (6–10 m s^{-1}). We used frond Reynolds number to extrapolate drag coefficients in the field and to predict water velocities necessary to break fronds of given sizes. Laboratory data successfully predicted frond sizes found in the field, suggesting that, although *Calliarthron* is well adapted to resist breakage, wave forces may ultimately limit the size of intertidal fronds.

Key words: adaptation, biomechanics, breaking stress, *Calliarthron*, decalcification, drag, flexibility, geniculum, intertidal, macroalgae, material properties.

INTRODUCTION

The intertidal zone of rocky shores is a hydrodynamically stressful environment, where breaking waves can generate water velocities greater than 25 m s^{-1} (e.g. Denny et al., 2003) and impose great forces on intertidal inhabitants (Koehl, 1984; Koehl, 1986; Carrington, 1990; Gaylord et al., 1994; Denny, 1995; Gaylord et al., 2001; Helmuth and Denny, 2003). The severity of wave-induced forces has been hypothesized to limit the maximum size to which intertidal organisms can grow (e.g. Denny et al., 1985; Gaylord et al., 1994; Denny, 1999). For example, unlike whales and giant kelps that live in deeper water, intertidal flora and fauna rarely exceed 0.5 m in any dimension (Denny et al., 1985). Blanchette found that intertidal algae transplanted from sheltered to wave-exposed locations 'tattered' back to a smaller size (Blanchette, 1997). Such damage is likely to be the result of drag, the primary wave-induced force applied to intertidal macroalgae (Denny and Gaylord, 2002).

Several studies have measured drag on seaweeds in an attempt to predict the size to which various species can grow in the intertidal zone (Carrington, 1990; Dudgeon and Johnson, 1992; Gaylord et al., 1994; Wolcott, 2007) but have had mixed success. This may be due in part to the characterization of drag at slow speeds (<3 m s^{-1}) in re-circulating water flumes and the need to extrapolate from these data to environmentally relevant water velocities (20–30 m s^{-1}). Such long-range extrapolations can be misleading (Vogel, 1994; Bell, 1999). In particular, drag coefficient (C_d) decreases as flexible macroalgae bend and reconfigure with increasing water velocity (Bell, 1999; Boller and Carrington, 2006a), but the extent of this reconfiguration and its effect on C_d have never been characterized at the high velocities found on wave-swept shores. Here, we introduce a gravity-accelerated water flume, capable of generating jets of water (meant to mimic crashing waves) up to 10 m s^{-1}. Thus, for the first time, it is possible to measure drag and re-configuration of seaweeds at high velocities, reducing the need for extrapolation.

The articulated coralline alga *Calliarthron cheilosporioides* Manza thrives in wave-swept intertidal habitats along the California coast (Abbott and Hollenberg, 1976). Unlike fleshy algae, which are flexible along their entire length, *Calliarthron* thalli are firmly calcified but have flexible joints (genicula) that allow fronds to bend when struck by breaking waves. Flexible genicula also define breakage points along calcified thalli (Martone, 2006) and are hypothesized to be especially susceptible to bending stresses, as segmented bending may locally amplify stress within genicula [see accompanying paper (Martone and Denny, 2008)]. Nevertheless, *Calliarthron* fronds can grow to a length of 25 cm, including more than 100 genicula, and can dominate the most wave-exposed habitats.

When struck by incoming waves, erect articulated fronds bend in the direction of flow parallel to the substratum. Most genicula are stretched in tension by each passing wave, but basal genicula, which are farthest from the free end of any frond, experience the greatest bending moments (see Martone and Denny, 2008) and are hypothesized to be the most prone to breakage (Martone, 2006). Morphological characteristics of bending genicula are significantly different from those of tensile genicula [see table 3 of the accompanying paper (Martone and Denny, 2008)], helping them increase flexibility and decrease stress amplification [see figure 7 of accompanying paper (Martone and Denny, 2008)], and bending angles may be constrained by the close proximity of neighboring

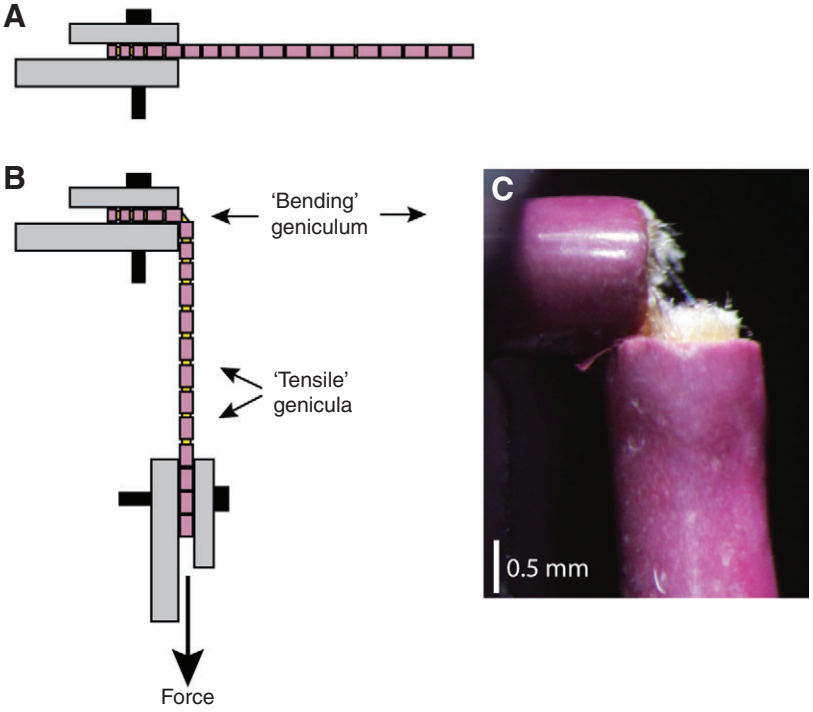

Fig. 1. Bend-to-break tests. (A) Articulated fronds were held between two clamps and (B) weights were hung from the free end until a geniculum broke. (C) Genicula did not rupture abruptly; instead, genicular cells ruptured and frayed sequentially with increasing force. Strain of intact tissue approached, but did not exceed, previously calculated breaking strains.

fronds, further mitigating the amplification of stress within bending genicula. The mechanical advantages of such traits may be limited, however, if tensile genicula ultimately break first.

In this study, we compared breaking forces of genicula and drag forces on articulated fronds to explore physical constraints on the size and survival of this ecologically successful intertidal seaweed. We used empirical and modeling techniques to quantify forces to break bending genicula, with and without neighbors, and compared them with forces sufficient to break tensile genicula. These data allowed us to evaluate the mechanical limits of bending genicula and to estimate the average drag force required to break fronds in the field. Drag on articulated fronds was measured in the lab, and the size to which fronds can grow without breaking in a given water velocity was predicted. We tested laboratory predictions by measuring maximum water velocities and frond sizes in the field and propose that, although articulated fronds are remarkably well adapted to resisting wave-induced drag, breaking waves may, indeed, be sufficient to constrain the size of intertidal *Calliarthron*.

MATERIALS AND METHODS

Material properties

Calliarthron fronds (N=15) were collected from the low intertidal zone in a moderately wave-exposed surge channel at Hopkins Marine Station (HMS) in Pacific Grove, CA, USA. Stress–strain curves were generated for one geniculum in each frond loaded in tension using a custom-made tensometer and a video dimension analyzer (model V94, Living Systems Instrumentation, Burlington, VT, USA) as described in the accompanying paper (Martone and Denny, 2008). Tensile moduli (E_t) were calculated as the slopes of linear stress–strain regressions forced through the origin; breaking strains (ε_{break}) were assumed to be the strain measurements immediately preceding frond breakage during mechanical tests. E_t and ε_{break} were correlated, and a linear regression was fitted to the E_t *versus* ε_{break} data. Residuals were calculated for each datapoint (N=15), and the standard deviation of residuals was calculated.

Bend-to-break tests

In the field, *Calliarthron* fronds often break near the base (Martone, 2006), where bending moments and bending stresses are greatest (Martone and Denny, 2008). To explore breakage in bending, *Calliarthron* fronds (N=7) were collected from the field site described above. Branches were removed from each frond by cutting below the first dichotomy, and the remaining straight chains of segments were tested as follows. Individual fronds were gripped in clamps by the first few genicula and held horizontal (Fig. 1A). To quantify the force to bend genicula to failure, a second clamp was secured near the tenth genicula (numbered from the clamp) and masses were hung, in 20 g and 50 g increments, from the clamp until fronds broke (Fig. 1B). As bending genicula experienced increasing force, they broke gradually (Fig. 1C). An image analysis revealed that unbroken genicular cells approached, but had not yet exceeded, the average breaking strain (ε_{break}) of genicula loaded in tension (P.T.M. and M.W.D., unpublished data).

Dimensions of broken genicula were quantified as described in figure 1 of the accompanying paper (Martone and Denny, 2008). Genicular radii (r_1, r_2) and intergenicular radii (y) were measured with an ocular dial-micrometer. Genicular lengths (ω) and gap lengths (ω–2x) were measured in wet, long-sectioned genicula adjacent to broken genicula and briefly decalcified in HCl. Average length measurements were assumed for broken genicula. Intergenicular lip length (x) of broken genicula was estimated as half the difference between mean ω and mean gap length.

Modeling breakage in bending

The mathematical model that we present in our other study (Martone and Denny, 2008) was augmented to allow genicula to break gradually in order to estimate the force to bend experimental genicula to failure. The distribution of breaking strains was assumed to be normal with a mean of $\bar{x}_{\varepsilon,break}$ and standard deviation of s.d.$_{\varepsilon,break}$, and when tensile moduli (E_t) were plotted against breaking strains (ε_{break}), residuals were assumed to be normally distributed around the linear regression with a mean of 0 and standard deviation of

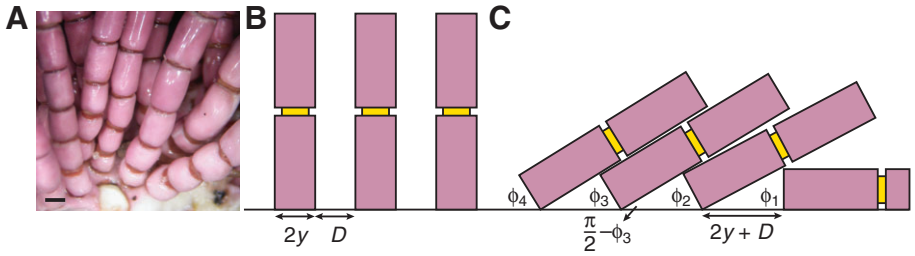

Fig. 2. (A) *Calliarthron* fronds grow in densely packed clusters. Depicted are several fronds emerging from crustose bases in the field. (B) Using the average diameter of basal intergenicula ($2y$) and distance between fronds (D), we calculated (C) the maximum bending angle (ϕ) of central fronds supported by neighbors. Note that frond spacing has been exaggerated for illustration purposes. Scale bar in A, 1 mm.

$s.d._{residual}$. To generate unique bivariate normal pairs of E_t and ε_{break} for each iteration of the model, a random value was chosen from the ε_{break} distribution and a corresponding E_t was calculated from the normal distribution of values around the regression. As virtual fronds deflected, the model eliminated any portion of the first geniculum whose strain exceeded ε_{break} (see Appendix). This reduction of tissue was factored into the internal moments and neutral axis positions calculated by the model. In some cases, reduction of genicular cross-section created a positive feedback, increasing bending angles and further increasing strain. Breakage occurred when $\varepsilon>\varepsilon_{break}$ across the entire geniculum. All other components of the original bending model were unchanged (see Martone and Denny, 2008).

To validate the model, forces (means ± s.d.) to break experimentally broken genicula described above (N=7) were estimated mathematically from 1000 model iterations. Observed and predicted breaking forces were compared.

Breaking force predictions

To estimate breakage of fronds in the field, morphological dimensions of 10 fronds were used from our other analysis [see table 3 in Martone and Denny (Martone and Denny, 2008)]. Forces to break first genicula (nearest the base) of these experimental fronds in bending were calculated from 1000 model iterations (means ± s.d.; N=10).

Calliarthron grow in dense clusters in the field, and fronds emerging from individual bases are tightly packed together (Fig. 2A). The spatial density of fronds probably limits bending angles of basal genicula. To evaluate this 'neighbor effect', the spatial density of fronds was measured in 15 *Calliarthron* individuals growing in the low intertidal zone at HMS. Average distance between fronds (D) was calculated from the average diameter of basal intergenicula ($2y$=1.334 mm) [see table 3 in Martone and Denny (Martone and Denny, 2008)] and the number of fronds growing within 1 cm of one another (N=15; Fig. 2B). Given average intergenicular diameter and spacing, the maximum bending angle (ϕ_i) of each frond depends upon the bending angle (ϕ_{i-1}) of the neighboring frond:

$$\phi_i = \frac{\pi}{2} - \arctan\left(\frac{2y\sin\phi_{i-1}}{2y + D - 2y\cos\phi_{i-1}}\right). \quad (1)$$

According to this equation, bending angles of articulated fronds equilibrate a few fronds within the periphery, assuming that fronds at the edge can bend 90 deg. (Fig. 2C). To evaluate the effect of this constraint on breaking force, the mathematical model was adjusted to prevent bending angles of first genicula from exceeding the mean bending angle of central fronds (i.e. positioned five neighbors within the periphery). Forces to break first genicula in the 10 experimental fronds (mean ± s.d.) with neighbors were calculated from 1000 model iterations. Forces to break fronds with and without neighbors were compared.

When fronds bend over, most genicula experience drag force in tension [see right panels of figure 4 in Martone and Denny (Martone and Denny, 2008)]. Tensile forces required to break tenth genicula in the 10 experimental fronds were estimated using genicular cross-sectional area and breaking stresses sampled from a normalized distribution with $\bar{x}_{\sigma,break}$=25.9 MN m^{-2} and $s.d._{\varepsilon,break}$=2.3 MN m^{-2} [determined by Martone (Martone, 2006)]. Mean and standard deviation of 1000 breaking force estimates were calculated for each geniculum. Forces to break tenth genicula in tension and to break first genicula in bending were compared, assuming fronds would break at the lesser force. Mean and standard deviation of forces to break fronds were calculated, and these values were used to predict breakage of articulated fronds in the field.

Drag force measurements

When intertidal algae are struck by breaking waves, drag can be calculated from the following equation:

$$F_{drag} = \frac{1}{2}\rho U^2 A C_d, \quad (2)$$

where ρ is seawater density (approximately 1025 kg m^{-3}), U is water velocity, A is algal planform area, and C_d is the drag coefficient, a dimensionless index of shape change and reconfiguration of flexible fronds (Carrington, 1990; Dudgeon and Johnson, 1992; Gaylord et al., 1994; Bell, 1999) (see also Boller and Carrington, 2006a).

To quantify the effect of frond size and growth on drag force, *Calliarthron* fronds (N=24) were collected from the low intertidal zone at HMS and were tested in re-circulating and gravity-accelerated water flumes. In both flume types, fronds were attached with cyano-acrylate glue to custom-made force transducers. In the re-circulating flume, drag force was measured on fronds (N=8) at 0.23, 0.46, 0.69, 0.92, 2.0 and 3.6 m s^{-1}. In the gravity-accelerated water flume, drag force was measured as fronds were struck with jets of water (Fig. 3). Flow was fully turbulent as it fell through the 10 cm diameter pipe, and velocity was adjusted by varying the distance through which the water fell. Fronds were tested at 6.8 m s^{-1} (N=6) and 10.0 m s^{-1} (N=10).

To explore changes in drag force over the lifetime of *Calliarthron*, fronds were 'de-grown' by sequentially removing apical branches, and the resulting effect on drag force was quantified. This method reasonably approximated *Calliarthron* ontogeny (in reverse), since most growth occurs at the apical meristem (Johansen, 1981) and genicula are approximately the same size in young and old fronds (Martone, 2007). Drag on whole fronds was measured, apical branches of fronds were removed, and drag force was re-measured. Then sub-apical branches of fronds were removed, and drag force was re-measured. This process was repeated until all branches had been removed. Severed branches were digitally photographed and planform areas were measured using an image analysis program (ImageJ, NIH Image, http://rsb.info.nih.gov/ij/). The correlation

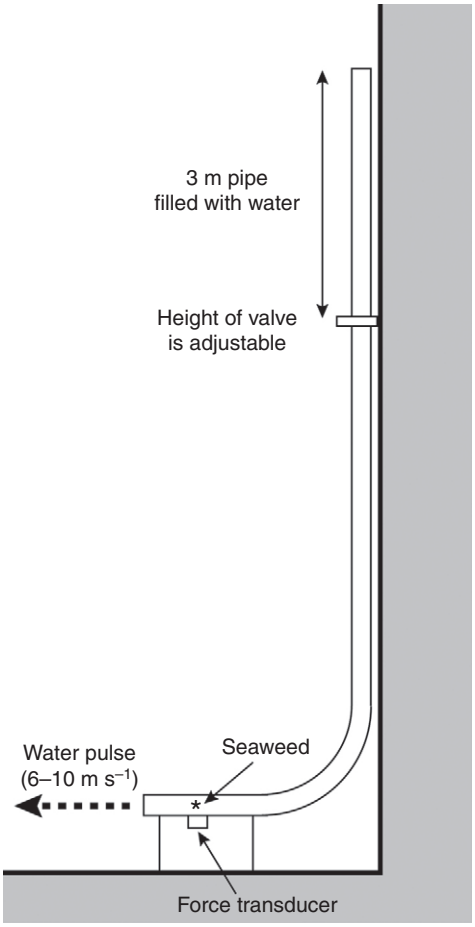

Fig. 3. Diagram of high-speed water flume. Water fell through a 10 cm diameter pipe that extended down the side of the building, creating jets of turbulent flow up to 10 m s^{-1}. *Calliarthron* fronds were attached to a force transducer in the working section, and drag was measured on fronds exposed to flow.

between frond planform area and drag force was plotted for fronds at all eight water velocities.

To compare the performance of *Calliarthron* fronds with that of streamlined bodies and fleshy algae in flow, Vogel's *E* (Vogel, 1984) was calculated as the slope of a linear regression fitted to a log–log plot of speed-specific drag (F_{drag}/U^2) *versus* velocity (U).

Calculating drag coefficients, C_d

Given drag force measurements, drag coefficients were calculated for every combination of frond planform area (A) and water velocity (U) by re-arranging Eqn 2:

$$C_d = \frac{2F_{drag}}{\rho U^2 A} . \quad (3)$$

Data revealed that drag coefficient decreased with both increasing velocity and increasing frond planform area, making extrapolations based on one parameter alone inaccurate. Instead, drag coefficient was plotted against frond Reynolds number, Re_f, a function of both velocity and area:

$$Re_f = \frac{U L}{\nu} = \frac{U\sqrt{A}}{\nu} , \quad (4)$$

where L is characteristic frond dimension (represented here by the square-root of A) and ν is the kinematic viscosity of water (1×10^{-6} m^2 s^{-1} at 20°C). Drag coefficients decreased with increasing Re_f according to the power curve:

$$\log C_d = a + b(\log Re_f)^{-c} . \quad (5)$$

Parameters a, b and c were estimated for the data using Matlab (v7.0.1, The Mathworks, Natick, MA, USA), and 95% confidence intervals (CI) around the fitted curve were calculated from 1000 bootstrapped datasets created by sampling with replacement of the original data (Efron and Tibshirani, 1993).

Drag force extrapolation

Re-arranging Eqn 4 and squaring both sides yields:

$$\nu Re_f = U\sqrt{A}$$
$$\nu^2 Re_f^2 = U^2 A . \quad (6)$$

By substituting Eqns 5 and 6 into the drag equation (Eqn 2), we obtain drag in terms of Re_f:

$$F_{drag} = \frac{1}{2}\rho U^2 A C_d$$
$$= \frac{1}{2}\rho\nu^2 Re_f^2 C_d$$
$$= \frac{1}{2}\rho\nu^2 Re_f^2 \{\exp[a + b(\log Re_f)^{-c}]\} . \quad (7)$$

F_{drag} was plotted against Re_f for all frond areas and velocities. Parameters a, b and c (calculated in Eqn 5) were used to plot a F_{drag} *versus* Re_f curve; 95% CI around this curve were calculated in Matlab by estimating parameters for the same 1000 bootstrapped $\log C_d$ *versus* $\log Re_f$ datasets and then calculating the range of F_{drag}.

Predicting breakage in the field

Fronds are expected to break in the field when drag force experienced by genicula exceeds breaking force. This expectation can be represented as follows:

$$F_{drag} = \frac{1}{2}\rho\nu^2 Re_f^2 \{\exp[a + b(\log Re_f)^{-c}]\} \geq F_{break} . \quad (8)$$

Critical frond Reynolds numbers ($Re_{f,crit}$) predicted to break genicula were calculated iteratively using Matlab. For the mean breakage prediction, $Re_{f,crit}$ was estimated using mean F_{break} and the mean F_{drag} *versus* Re_f curve. For the best case scenario, $Re_{f,crit}$ was estimated using mean F_{break}+s.d. and the mean curve –95% CI. For the worst case scenario, $Re_{f,crit}$ was estimated using mean F_{break}–s.d. and the mean curve +95% CI. Then, using Eqn 4, we explored the combinations of velocity (U) and frond area (A) that would yield each critical Re_f. U *versus* A curves were plotted for each $Re_{f,crit}$ and were used to predict the maximum area to which fronds could grow in a given water velocity or, conversely, the minimum water velocity necessary to break fronds of a given size:

$$U = \frac{Re_{f,crit}\,\nu}{\sqrt{A}} . \quad (9)$$

Field measurements

From November 2003 to November 2006, *Calliarthron* fronds were collected every few months, totaling eight collections, from the intertidal field site described above. During each collection we

searched for the largest available fronds. Collections typically consisted of 10–20 fronds. Fronds were digitally photographed and frond planform areas were measured using image analysis (ImageJ). Maximum frond area was noted on each date over the 3 year span.

From November 2005 to August 2006, maximum water velocities were measured. On 2 November 2005, three dynamometers (Bell and Denny, 1994; Helmuth and Denny, 2003) were installed at mean lower low water approximately 0.75 m apart, spanning the field site. Dynamometers were first checked and reset on 4 November 2005 and were checked and reset during sufficiently low tides (13 times) until 10 August 2006. The maximum water velocity recorded by any dynamometer was noted on each date over the 9 month span.

Field measurements were compared with breakage predictions to determine whether water velocities in the field were sufficient to generate drag forces that would equal forces experimentally determined to break *Calliarthron* fronds.

RESULTS

Material properties

Mean ε_{break} of genicula was 1.18±0.44 (mean ± s.d.), and mean E_t of genicula was 27.7±12.4 MN m^{-2} (mean ± s.d.). ε_{break} and E_t were significantly negatively correlated (Fig. 4; R^2=0.62, P<0.001), such that:

$$E_t = (-22.0\varepsilon_{break} + 53.7)\times 10^6 . \quad (10)$$

Standard deviation of residuals around the regression was 7.7 MN m^{-2}.

Bend-to-break tests and model validation

Predicted and observed breaking forces were similar (Table 1) and, on average, were not significantly different (P=0.47, Student's paired t-test).

Breaking force predictions

Without neighbors, bending genicula were predicted to break before tensile genicula because, on average, tensile genicula resisted significantly more force (P<0.01, paired t-test; Fig. 5). However, fronds were predicted to resist greater forces in bending when supported by neighboring fronds (Fig. 5). Neighboring fronds were spaced 0.4 mm apart, on average, limiting bending angles to approximately 54 deg. With neighbors, bending genicula and tensile genicula were predicted to resist similar forces (Fig. 5), which, on average, were not significantly different (P=0.30, paired t-test). Mean force to break first genicula in bending with neighbors was 26.3 N, and the mean force to break tenth genicula in tension was 22.7 N (Table 2). Assuming fronds would break at the lesser of the two breaking forces for each frond, mean force to break *Calliarthron* fronds was 20.0±3.8 N (mean ± s.d.; Table 2).

Table 1. Comparison of observed and predicted forces (means ± s.d.) to experimentally break *Calliarthron* genicula in bending

Frond	Observed (N)	Predicted (N)
1	9.3	10.3±3.4
2	9.5	8.8±2.7
3	7.5	15.8±4.9
4	14.4	8.0±2.8
5	14.4	11.0±3.9
6	11.0	6.7±2.4
7	12.0	7.2±2.5

Drag force measurements and drag coefficient estimates

For all water velocities, drag force increased with frond planform area, and fronds of any given area experienced more drag force at greater velocities (Fig. 6). Vogel's E was calculated to be –0.68 (R^2=0.70; Fig. 7).

Drag coefficients decreased with increasing water velocity and increasing frond area (Fig. 8). Given its dependence on both frond area and water velocity, drag coefficient decreased with increasing frond Reynolds number (Fig. 9). The following curve captured nearly all of the variation in the data (R^2=0.95):

$$\log C_d = -2.06 + 223.24(\log \mathrm{Re_f})^{-3.58} . \quad (11)$$

Predicting drag and breakage in the field

Drag was plotted against frond Reynolds number (Fig. 10):

$$F_{drag} = \frac{1}{2}\rho v^2 \mathrm{Re_f}^2 \{\exp[-2.06 + 223.24(\log \mathrm{Re_f})^{-3.58}]\} . \quad (12)$$

Using Eqn 12 and associated 95% CI (see Materials and methods), $\mathrm{Re_{f,crit}}$ was calculated for F_{drag}=F_{break} (determined to be 20.0±3.8 N,

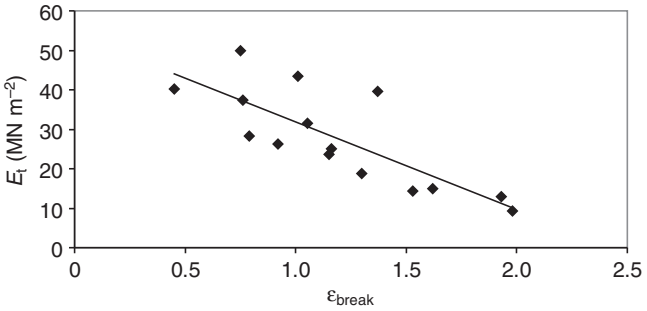

Fig. 4. Correlation between tensile modulus (E_t) and breaking strain (ε_{break}) of individual genicula.

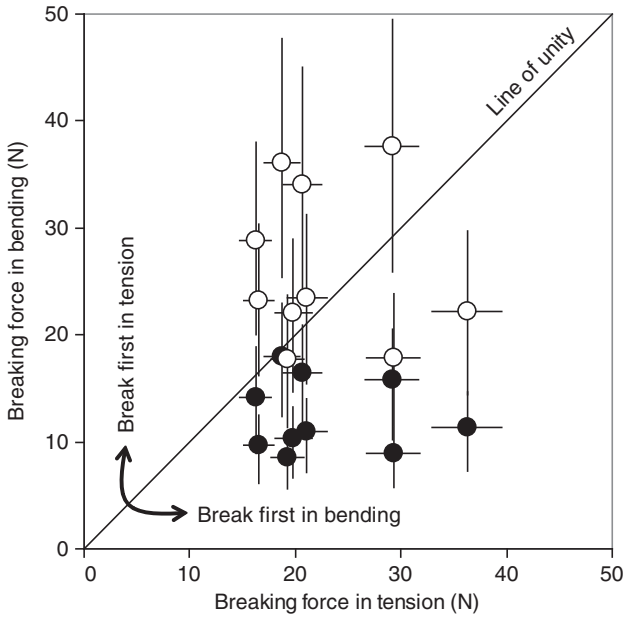

Fig. 5. Forces (±s.d.) predicted to break tenth genicula in tension and first genicula in bending for 10 experimental fronds. Without neighbors (filled circles), fronds are more likely to break in bending at first genicula. With neighbors (open circles), fronds may break in tension or in bending.

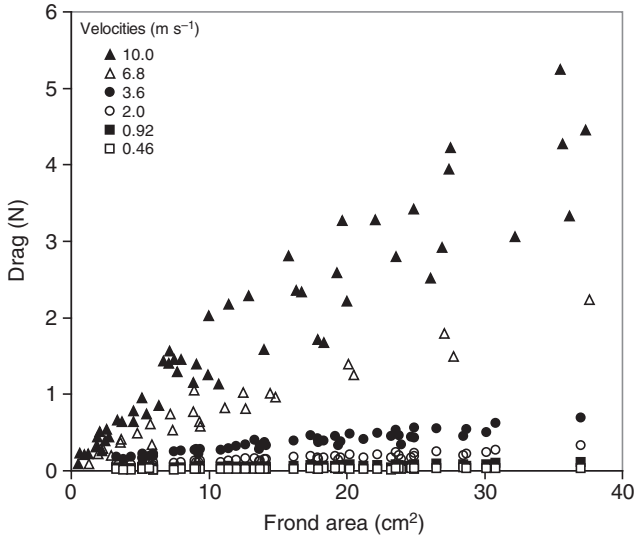

Fig. 6. Effect of frond planform area on drag force. Data are presented for all fronds at six representative velocities.

Table 2. Summary of forces predicted to break experimental fronds

Frond	First geniculum in bending (N)	Tenth geniculum in tension (N)
1	36.1	**18.7**
2	34.0	**20.7**
3	23.5	**21.1**
4	**17.7**	19.2
5	28.8	**16.2**
6	22.0	**19.8**
7	**17.8**	29.3
8	23.2	**16.5**
9	**22.2**	36.3
10	37.6	**29.2**
Mean	26.3	22.7
Mean break force ± s.d.	20.0±3.8	

Numbers in bold indicate the geniculum predicted to break first in each pair.

mean ± s.d.). For F_{break}=16.2 N (mean−1 s.d.), $Re_{f,crit}=1.15\times10^6$; for F_{break}=20.0 N (mean), $Re_{f,crit}=1.45\times10^6$; for F_{break}=23.8 N (mean+1 s.d.), $Re_{f,crit}=1.89\times10^6$ (Fig. 10).

Substituting these values for $Re_{f,crit}$ in Eqn 9, the following three equations were generated to predict water velocities that would break fronds of given planform area in the field (Fig. 11):

$$U=\frac{\left(1.15\times10^6\right)\nu}{\sqrt{A}}$$

$$U=\frac{\left(1.45\times10^6\right)\nu}{\sqrt{A}}$$

$$U=\frac{\left(1.89\times10^6\right)\nu}{\sqrt{A}}\ , \qquad (13)$$

corresponding to F_{break}=16.2, 20.0 and 23.8 N, respectively. Larger fronds were predicted to break at slower water velocities. Fronds smaller than 10 cm^2 were predicted to resist water velocities greater than 40 $m\,s^{-1}$.

The greatest water velocity recorded at the field site was 22.1 $m\,s^{-1}$ (Table 3). On average, the largest frond collected from the field site was 40.9±7.8 cm^2 (mean ± s.d.), and the largest frond ever collected from the site was 51.9 cm^2 (Table 4). These field measurements corresponded well to breakage predictions (Fig. 11).

DISCUSSION

Optimized to resist breakage

Despite the amplification of bending stresses within genicular tissue (Martone and Denny, 2008), *Calliarthron* genicula are clearly well adapted to resist mechanical failure in wave-swept habitats. Even without the support of neighbors, fronds located near the periphery of aggregations are able to bend to 90 deg., and several experimental fronds supported more than 1 kg of weight (>9.8 N) in this position (Table 1). When neighboring fronds are considered, bending angles of central fronds are constrained, allowing first genicula to resist approximately twice the force of fronds near the periphery. Ultimately, fronds growing within dense populations are just as likely to break at tenth genicula in tension as they are to break at first genicula in bending.

These data suggest that genicula are not 'over-designed' in an evolutionary sense. The tensile strength of calcified intergenicula in *Calliarthron* (28.5 $MN\,m^{-2}$) (Martone, 2006) is similar to that of coral skeleton (25.6 $MN\,m^{-2}$) (Vosburgh, 1982) and to that of several bivalve and gastropod shells that appear similar to *Calliarthron* cell walls ('homogeneous' type, 30 $MN\,m^{-2}$; 'foliated' type, 38.3 $MN\,m^{-2}$) (Currey, 1980). This suggests an upper limit to the tensile strength of biologically deposited calcium carbonate within *Calliarthron* cell walls. This mechanical constraint may be biologically linked to genicula, whose tissue is equally strong (25.9 $MN\,m^{-2}$) (Martone, 2006). Indeed, genicular tissue is far stronger than other algal tissues (up to an order of magnitude) (Martone, 2006) but may be biologically

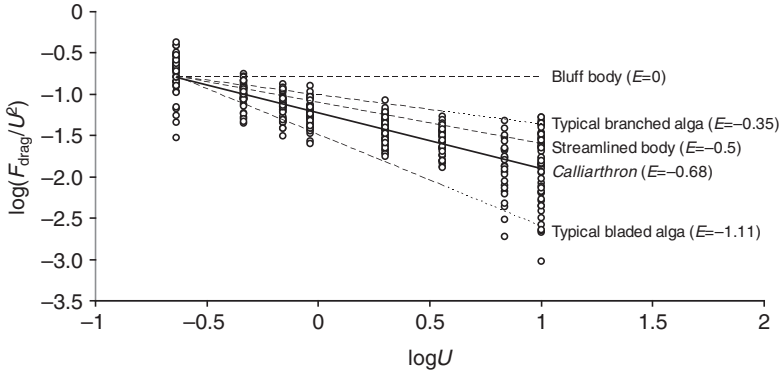

Fig. 7. Speed-specific drag (F_{drag}/U_2) as a function of water velocity (U). Slopes of the linear regressions are Vogel's E values. *Calliarthron* data are represented by circles and solid line; all other data (E values and dashed lines) were compiled from studies by Vogel, and Gaylord and colleagues (Vogel, 1994; Gaylord et al., 1994). Data suggest that the drag coefficient of *Calliarthron* drops faster than that of a streamlined body, but not as fast as that of a typical bladed alga. Because of limitations of re-circulating flumes used in past studies, Vogel's E has not yet been properly characterized for other intertidal algae at high water velocities (6–10 $m\,s^{-1}$; dotted lines).

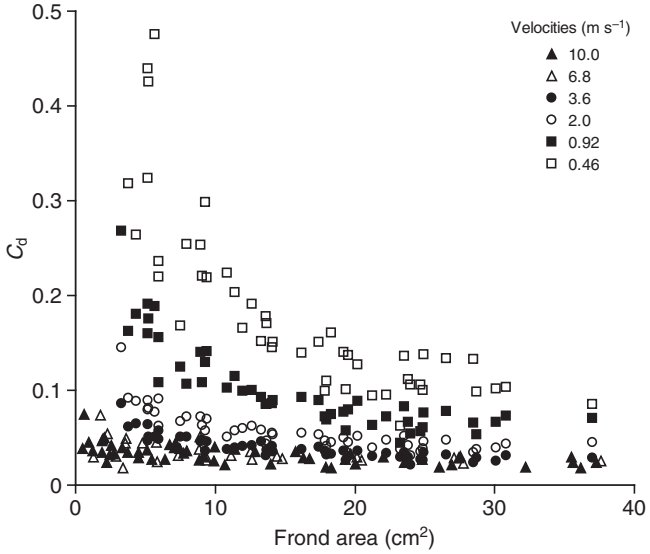

Fig. 8. Effect of frond planform area on drag coefficient (C_d). Data are presented for all fronds at six representative velocities. Note that drag coefficient varied with both water velocity and frond planform area.

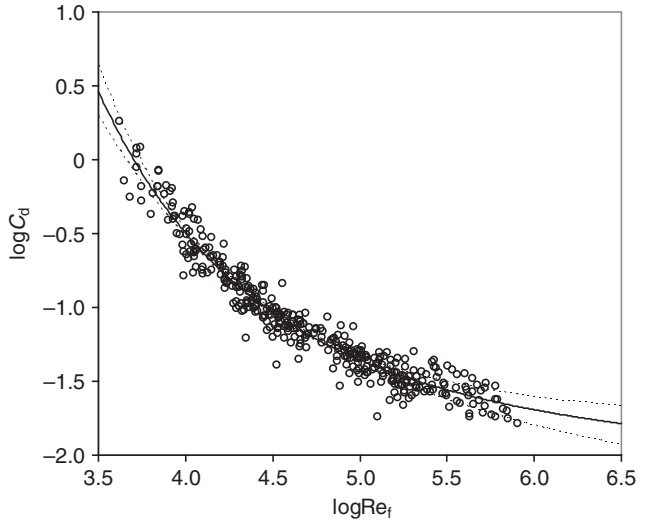

Fig. 9. Drag coefficient decreased with frond Reynolds number (Re_f), a function of both velocity and area. Dotted lines represent 95% CI around the fitted model.

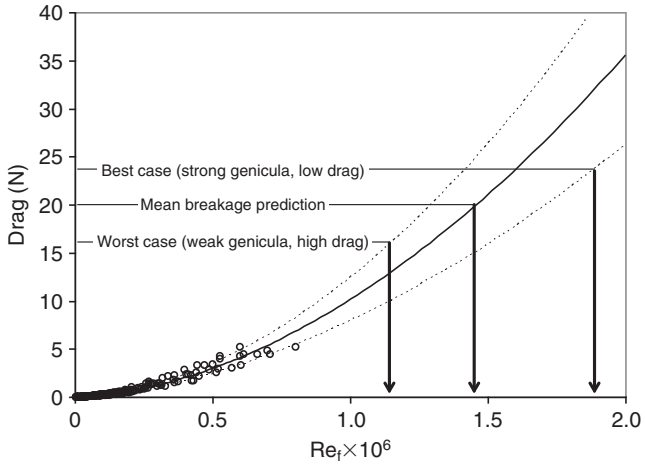

Fig. 10. Drag force increased with frond Reynolds number. The curve was fitted to data generated in the lab (circles); dotted lines represent 95% CI. Mean, best case and worst case scenarios, based on mean F_{break} ± 1 s.d., indicate the Re_f expected to break fronds in the field.

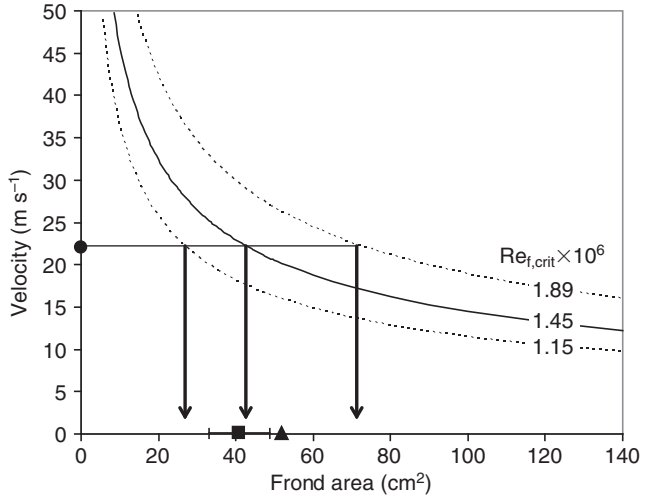

Fig. 11. Velocities predicted to break fronds of a given planform area (critical frond Reynolds number, $Re_{f,crit}$). Dotted lines represent 95% CI around the model prediction, based on mean F_{break} ± s.d. Maximum water velocity measured in the field (circle) successfully predicts the mean maximum size (±s.d.; square) of *Calliarthron* fronds expected to survive. The size of the largest frond (triangle) suggests that water velocities at the field site may exceed those measured during this experiment (see text).

constrained from growing any stronger. Given this putative maximum tensile strength of genicular tissue, there may not be a selective advantage to adjusting the spatial density of fronds or the dimensions of bending genicula, if tensile genicula would ultimately break first. In other words, growing more densely packed clusters of fronds or decreasing the length of intergenicula (see Martone and Denny, 2008) may indeed increase the breaking force of bending genicula, but such fronds would probably break at tensile genicula anyway; and breakage of either bending or tensile genicula near the base is likely to be disadvantageous, resulting in the loss of an entire frond that may have been reproductive and several years old (Johansen and Austin, 1970).

Together, these data are consistent with the engineering theory of optimal design [Maxwell's Lemma (see Wainwright et al., 1982)], which states that all components in a mechanically stressed system should be equally strong to avoid wasting resources in their construction. The fact that bending and tensile genicula are morphologically distinct (Martone and Denny, 2008) but resist similar drag forces suggests that these structures may have been shaped by selective pressures imposed by breaking waves. Morphological differences among tensile and bending genicula, therefore, may represent adaptations to hydrodynamic stress.

Environmentally relevant drag coefficient

To our knowledge, this is the first study to report drag coefficients for an intertidal seaweed at high, environmentally relevant water velocities. Drag coefficients reported here for *Calliarthron* are up to an order of magnitude lower than those reported for several other algae at slow water velocities (Carrington, 1990; Dudgeon and

Table 3. Maximum water velocities recorded by dynamometers at field site

Date	Maximum water velocity ($m s^{-1}$)
4 Nov 05	11.2
15 Nov 05	13.6
16 Nov 05	22.1
30 Nov 05	12.0
13 Dec 05	11.6
29 Dec 05	12.2
24 Feb 06	9.6
24 Mar 06	18.6
15 May 06	8.3
30 May 06	9.0
13 Jun 06	7.3
26 Jun 06	9.6
10 Aug 06	7.3
Overall maximum	22.1

Table 4. Maximum size of *Calliarthron* fronds collected on given dates

Date	Maximum frond size (cm^2)
23 Nov 03	34.3
21 Jan 04	26.9
5 Jul 04	44.3
17 Jan 05	51.9
8 Feb 05	47.7
13 Dec 05	42.8
26 Jun 06	39.4
4 Nov 06	39.9
Mean ± s.d.	40.9±7.8
Overall maximum	51.9

Johnson, 1992; Gaylord et al., 1994). Our data suggest that drag coefficient continues to decrease as water velocity increases, at least up to $6 m s^{-1}$ (Fig. 8), contrary to the assumption that reconfiguration is solely a low-velocity phenomenon (see Bell, 1999). Vogel's E (–0.68) suggests that the drag coefficient of reconfiguring *Calliarthron* fronds drops faster than that of a typical streamlined body (–0.50) (Vogel, 1984) and faster than those of several branched red algae, including a congeneric species (–0.35±0.13, mean ± s.d., N=7 species), although slower than those of flat bladed algae (–1.11±0.10, N=3 species; Fig. 7) [data compiled from table 4 in Gaylord et al. (Gaylord et al., 1994)]. Without high-speed data for other seaweeds, it is unknown at this time whether such low drag coefficients are a distinct characteristic of *Calliarthron* or a shared feature of intertidal algae. Our data emphasize the importance of measuring drag at high water velocities to avoid, or at least improve, extrapolation. For example, Gaylord and colleagues extrapolated fivefold beyond their data to generate drag predictions (Gaylord et al., 1994); in contrast, we would need to extrapolate less than twofold beyond our high-speed flume velocities (i.e. a short distance along the $\log Re_f$ axis of Fig. 9) to generate the same predictions. The accuracy of past predictions awaits verification in the high-speed flume.

Our data demonstrate effects of both planform area and water velocity on drag coefficient, suggesting yet another source of error in previous studies that treated drag coefficient strictly as a function of velocity and tested only a narrow size range of fronds (e.g. Carrington, 1990; Dudgeon and Johnson, 1992; Gaylord et al., 1994; Bell, 1999). Flexible algal fronds have lower drag coefficients in faster water because of the increased reconfiguration that occurs as fronds bend. Similarly, larger fronds are likely to have lower drag coefficients because of their capacity to re-arrange their branches and collapse to be more streamlined, unlike smaller fronds whose sparse branches are perhaps less capable of reconfiguration (Fig. 8).

It is important to note that, in this and previous studies of algal reconfiguration, drag coefficient is calculated using frond planform area (i.e. flattened and photographed from above). This methodology assumes a constant area term, allowing the drag coefficient to absorb any change in shape due to reconfiguration; all else being equal, larger fronds will tend to have lower drag coefficients (see Eqn 3). This contrasts sharply with a recent study (Boller and Carrington, 2006a) that calculated drag coefficients using frond projected area (i.e. photographed from upstream in flow) and tracked the independent decline of both projected area and drag coefficient as macroalgae reconfigured with increasing water velocity – a method that had previously been applied to reconfiguring gorgonians (Sponaugle and LaBarbera, 1991). Their data show that as flow increases, projected areas and drag coefficients both decline; fronds with larger projected areas have higher drag coefficients. Unlike our method, theirs generates drag coefficients that are directly comparable to other engineering shapes. However, because projected area cannot be visualized or measured in turbulent water at high speeds (e.g. in the gravity-accelerated water flume or under breaking waves), predictions of projected area, like those for drag coefficient, will inevitably rely upon long-range extrapolations. Thus, even though the drag coefficients presented here cannot be compared with those of standard shapes, our method reduces extrapolation and so seems suited to exploring the maximum size to which wave-swept fronds can grow.

Limits to frond size in the intertidal zone

Forces estimated to break *Calliarthron* fronds in the field are consistent with forces previously measured to break genicula in tension (Martone, 2006). An average *Calliarthron* frond can resist approximately 20 N of force before breaking – a substantial amount of force. For example, one large experimental frond ($30 cm^2$) experienced only 5 N of drag force at $10 m s^{-1}$ (Fig. 6) – far below the threshold breaking force. This suggests that *Calliarthron* may be well adapted to resist drag imposed by intertidal water velocities. However, velocities as high as $35 m s^{-1}$ have been recorded at HMS (M.W.D., unpublished data), and articulated fronds may ultimately be size limited when water velocities approach this extreme.

Indeed, data presented here suggest that the size of *Calliarthron* fronds may be limited by drag forces imposed by intertidal water velocities. According to our breakage model, the maximum water velocity measured at the field site ($22.1 m s^{-1}$) closely predicts the mean maximum size (40.9±7.8 cm^2, mean ± s.d.) of *Calliarthron* fronds expected to survive there (Fig. 11). These data suggest that the broad range of frond sizes observed at the field site may, at least in part, be a consequence of variation in forces to break genicula. Our simplified breakage model ignores any possible drag-reducing effects of neighboring algae (Boller and Carrington, 2006b) and, because intertidal water velocities vary widely in both space and time (Denny and Wethey, 2001; Helmuth and Denny, 2003; O'Donnell, 2005), characterizing years of wave-forces with only a few dynamometer measurements is a broad generalization. For example, if breaking waves during some storm event actually generated $28 m s^{-1}$ water velocities at the field site – a distinct possibility – then the size of the largest frond predicted to survive, including 95% model error, would closely match the observed size

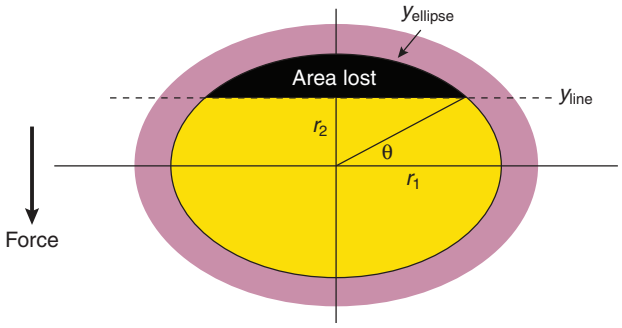

Fig. A1. Method used by bending model to calculate the proportion of cross-sectional area lost in geniculum (shown in black) during rupture. Remaining genicular tissue is shown in yellow; intergenicular tissue is shown in pink. *r*, genicular radii; *y*, intergenicular radii.

of the largest frond (51.9 cm^2; Fig. 11). The close correlation between maximum velocity and frond size across the field site suggests that, although *Calliarthron* is well adapted to resisting breakage, growth may ultimately be limited by wave-induced drag forces. Observations of larger fronds growing subtidally (K. A. Miller, personal communication), where drag is lower, support this conclusion but have yet to be properly quantified.

APPENDIX

Each iteration of the mathematical model accounted for breakage in the first geniculum by subtracting the portion of genicular cross-sectional area that had exceeded ε_{break}. After calculating frond deflection, the model determined the position within the geniculum, θ_{max}, where $\varepsilon=\varepsilon_{break}$ and subtracted the genicular area where $\theta>\theta_{max}$ (and therefore $\varepsilon>\varepsilon_{break}$; Fig. A1):

$$\begin{aligned}\text{Area lost} &= 2\int_0^x \left(y_{\text{ellipse}} - y_{\text{line}}\right)\mathrm{d}x \\ &= 2\int_{\frac{\pi}{2}}^{\theta_{\max}} \left(r_2\sin\theta - r_2\sin\theta_{\max}\right)\left(-r_1\sin\theta\right)\mathrm{d}\theta \\ &= 2\int_{\frac{\pi}{2}}^{\theta_{\max}} \left(r_1 r_2\sin\theta_{\max}\sin\theta - r_1 r_2\sin^2\theta\right)\mathrm{d}\theta \\ &= 2r_1 r_2\left[-\sin\theta_{\max}\cos\theta - \left(\frac{1}{2}\theta - \frac{1}{4}\sin 2\theta\right)\right]\Bigg|_{\frac{\pi}{2}}^{\theta_{\max}} \\ &= 2r_1 r_2\left(\frac{\pi}{4} + \frac{1}{4}\sin 2\theta_{\max} - \sin\theta_{\max}\cos\theta_{\max} - \frac{1}{2}\theta_{\max}\right).\end{aligned} \tag{A1}$$

This manuscript benefited from comments made by M. Boller, K. Mach, L. Miller, K. Miklasz, R. Martone, and two anonymous reviewers. Research was supported by the Phycological Society of America, the Earl and Ethyl Myers Oceanographic and Marine Biology Trust, and NSF grant no. IOS-0641068 to M.W.D. This is contribution number 309 from PISCO, the Partnership for Interdisciplinary Studies of Coastal Oceans, funded primarily by the Gordon and Betty Moore Foundation and the David and Lucile Packard Foundation.

REFERENCES

Abbott, I. A. and Hollenberg, G. J. (1976). *Marine Algae of California*. Stanford, CA: Stanford University Press.
Bell, E. C. (1999). Applying flow tank measurements to the surf zone: predicting dislodgment of the Gigartinaceae. *Phycological Res.* **47**, 159-166.
Bell, E. C. and Denny, M. W. (1994). Quantifying 'wave exposure': a simple device for recording maximum velocity and results of its use at several field sites. *J. Exp. Mar. Biol. Ecol.* **181**, 9-29.
Blanchette, C. A. (1997). Size and survival of intertidal plants in response to wave action: a case study with *Fucus gardneri*. *Ecology* **78**, 1563-1578.
Boller, M. L. and Carrington, E. (2006a). The hydrodynamic effects of shape and size change during reconfiguration of a flexible macroalga. *J. Exp. Biol.* **209**, 1894-1903.
Boller, M. L. and Carrington, E. (2006b). *In situ* measurements of hydrodynamic forces imposed on *Chondrus crispus* Stackhouse. *J. Exp. Mar. Biol. Ecol.* **337**, 159-170.
Carrington, E. (1990). Drag and dislodgement of an intertidal macroalga: consequences of morphological variation in *Mastocarpus papillatus* Kutzing. *J. Exp. Mar. Biol. Ecol.* **139**, 185-200.
Currey, J. D. (1980). Mechanical properties of mollusc shell. *Symp. Soc. Exp. Biol.* **34**, 75-78.
Denny, M. W. (1995). Predicting physical disturbance: mechanistic approaches to the study of survivorship on wave-swept shores. *Ecol. Monogr.* **65**, 371-418.
Denny, M. W. (1999). Are there mechanical limits to size in wave-swept organisms? *J. Exp. Biol.* **202**, 3463-3467.
Denny, M. W. and Gaylord, B. (2002). The mechanics of wave-swept algae. *J. Exp. Biol.* **205**, 1355-1362.
Denny, M. W. and Wethey, D. (2001). Physical processes that generate patterns in marine communities. In *Marine Community Ecology* (ed. M. D. Bertness, S. Gaines and M. E. Hay). Sunderland, MA: Sinauer Associates.
Denny, M. W., Daniel, T. L. and Koehl, M. A. R. (1985). Mechanical limits to size in wave-swept organisms. *Ecol. Monogr.* **55**, 69-102.
Denny, M. W., Miller, L. P., Stokes, M. D., Hunt, L. J. H. and Helmuth, B. S. T. (2003). Extreme water velocities: topographical amplification of wave-induced flow in the surf zone of rocky shores. *Limnol. Oceanogr.* **48**, 1-8.
Dudgeon, S. R. and Johnson, A. S. (1992). Thick vs. thin: thallus morphology and tissue mechanics influence differential drag and dislodgement of two co-dominant seaweeds. *J. Exp. Mar. Biol. Ecol.* **165**, 23-43.
Efron, B. and Tibshirani, R. J. (1993). *An Introduction to the Bootstrap*. New York: Chapman & Hall/CRC.
Gaylord, B., Blanchette, C. A. and Denny, M. W. (1994). Mechanical consequences of size in wave-swept algae. *Ecol. Monogr.* **64**, 287-313.
Gaylord, B., Hale, B. B. and Denny, M. W. (2001). Consequences of transient fluid forces for compliant benthic organisms. *J. Exp. Biol.* **204**, 1347-1360.
Helmuth, B. and Denny, M. W. (2003). Predicting wave exposure in the rocky intertidal zone: do bigger waves always lead to larger forces? *Limnol. Oceanogr.* **48**, 1338-1345.
Johansen, H. W. (1981). *Coralline Algae, A First Synthesis*. Boca Raton: CRC Press.
Johansen, H. W. and Austin, L. F. (1970). Growth rates in the articulated coralline *Calliarthron* (Rhodophyta). *Can. J. Bot.* **48**, 125-132.
Koehl, M. A. R. (1984). How do benthic organisms withstand moving water? *Am. Zool.* **24**, 57-70.
Koehl, M. A. R. (1986). Seaweeds in moving water: form and mechanical function. In *On the Economy of Plant Form and Function* (ed. T. J. Givnish), pp. 603-634. Cambridge: Cambridge University Press.
Martone, P. T. (2006). Size, strength and allometry of joints in the articulated coralline *Calliarthron*. *J. Exp. Biol.* **209**, 1678-1689.
Martone, P. T. (2007). Kelp versus coralline: cellular basis for mechanical strength in the wave-swept seaweed *Calliarthron* (Corallinaceae, Rhodophyta). *J. Phycol.* **43**, 882-891.
Martone, P. T. and Denny, M. W. (2008). To bend a coralline: effect of joint morphology on flexibility and stress amplification in an articulated calcified seaweed. *J. Exp. Biol.* **211**, 000-000.
O'Donnell, M. (2005). *Habitats and Hydrodynamics on Wave-Swept Rocky Shores*, pp. 152. Stanford, CA: Stanford University Press.
Sponaugle, S. and LaBarbera, M. (1991). Drag-induced deformation: a functional feeding strategy in two species of gorgonians. *J. Exp. Mar. Biol. Ecol.* **148**, 121-134.
Vogel, S. (1984). Drag and flexibility in sessile organisms. *Am. Zool.* **24**, 37-44.
Vogel, S. (1994). *Life in Moving Fluids*. Princeton, NJ: Princeton University Press.
Vosburgh, F. (1982). *Acropora reticulata*: structure, mechanics and ecology of a reef coral. *Proc. R. Soc. Lond., B, Biol. Sci.* **214**, 481-499.
Wainwright, S. A., Biggs, W. D., Currey, J. D. and Gosline, J. M. (1982). *Mechanical Design in Organisms*. Princeton, NJ: Princeton University Press.
Wolcott, B. D. (2007). Mechanical size limitation and life-history strategy of an intertidal seaweed. *Mar. Ecol. Prog. Ser.* **338**, 1-10.